Title: Rapid and Active Stabilization of Visual Cortical Firing Rates Across Light-Dark Transitions

Abbreviated Title: V1 Firing Rates Are Stable Across Light Transitions

Authors: Alejandro Torrado Pacheco*[1], Elizabeth I. Tilden*[1], Sophie M. Grutzner*[1], Brian J. Lane[1], Yue Wu[2], Keith B. Hengen[1], Julijana Gjorgjieva[2,3], Gina G. Turrigiano[1]

Author affiliations

1. Dept of Biology, Brandeis University, Waltham, MA 02453, USA

2. Max Planck Institute for Brain Research, 60438 Frankfurt, Germany

3: Technical University of Munich, School of Life Sciences, 85354 Freising, Germany

*: These authors (A.T.P., E.I.T., S.M.G.) contributed equally to this work.

Corresponding author: Correspondence should be addressed to: Gina G. Turrigiano, Dept of Biology, MS008, Brandeis University, 415 South St, Waltham, MA 02453, USA.

turrigiano@brandeis.edu

Number of pages: 50

Number of figures: 8

Number of words: Abstract: 250; Introduction: 650; Discussion: 1268

1

1   **Abstract**

2   The dynamics of neuronal firing during natural vision are poorly

3   understood. Surprisingly, mean firing rates of neurons in primary visual cortex (V1) of

4   freely behaving rodents are similar during prolonged periods of light and darkness, but it

5   is unknown whether this reflects a slow adaptation to changes in natural visual input, or

6   insensitivity to rapid changes in visual drive. Here we use chronic electrophysiology in

7   freely behaving rats of either sex to follow individual V1 neurons across many dark-light

8   (D-L) and light-dark (L-D) transitions. We show that, even on rapid timescales (1s to 10

9   min), neuronal activity was only weakly modulated by transitions that coincided with the

10   expected 12h/12h light-dark cycle. In contrast, a larger subset of V1 neurons consistently

11   responded to unexpected L-D and D-L transitions, and disruption of the regular L-D

12   cycle with 60 hours of complete darkness induced a robust increase in V1 firing upon re-

13   introduction of visual input. Thus, V1 neurons fire at similar rates in the presence or

14   absence of natural stimuli, and significant changes in activity arise only transiently in

15   response to unexpected changes in the visual environment. Further, although mean rates

16   were similar in L and D, pairwise correlations were significantly stronger during natural

17   vision, suggesting that information about natural scenes in V1 is more readily extractable

18   from correlations than from individual firing rates. Together, our findings show that V1

19   firing rates are rapidly and actively stabilized during expected changes in visual input,

20   and are remarkably stable at both short and long timescales.

21

Significance Statement

The firing dynamics of neurons in primary visual cortex (V1) are poorly understood. Indeed, V1 neurons of freely behaving rats fire at the same mean rate in light and darkness. It is unclear how this stability is maintained, and whether it is important for sensory processing. We find that transitions between light and darkness happening at expected times have only modest effects on V1 activity. In contrast, both unexpected transitions and light re-exposure after extended darkness robustly increase V1 firing. Finally, pairwise correlations in neuronal spiking are significantly higher during the light, when natural vision is occurring. These data show that V1 firing is remarkably stable, and that neuronal correlations may represent sensory information better than mean firing rates.

Introduction

Neurons in the cerebral cortex are spontaneously active, but the function of this internally generated activity is largely unexplained. Ongoing activity has been proposed to be noise due to random fluctuations (Zohary et al., 1994; Shadlen and Newsome, 1998; Averbeck et al., 2006). However other experiments have shown that spontaneous activity possesses coherent spatio-temporal structure (Arieli et al., 1995; Tsodyks et al., 1999; Ch'ng and Reid, 2010), suggesting it may play an important role in the processing of natural sensory stimuli (Arieli et al., 1995; Kenet et al., 2003; Fiser et al., 2004; MacLean et al., 2005; Luczak et al., 2009, 2013). In primary visual cortex (V1), spontaneous activity observed in complete darkness is similar to that evoked by visual stimulation with random noise stimuli, and is only subtly modulated by natural scene viewing (Gallant et al., 1998; Fiser et al., 2004). Recently we showed that individual V1 neurons have very stable mean firing rates in freely behaving rodents, and that these mean rates are indistinguishable in light and dark when averaged across many hours (Hengen et al., 2016). How V1 firing can be stable across such drastic changes in the visual environment while still meaningfully encoding sensory stimuli, and whether this stability is actively maintained or simply arises from intrinsic circuit dynamics, remains unknown.

Regulation of individual firing rates around a stable set point is thought to be essential for proper functioning of cortical circuits in the face of developmental or experience-dependent perturbations to connectivity (Miller and MacKay, 1994; Turrigiano and Nelson, 2004). Long-term stability of individual mean firing rates has now been observed in rodent V1 (Hengen et al., 2013, 2016; Keck et al., 2013) and M1 (Dhawale et al., 2017), suggesting it is a general feature of neocortical networks; further,

4

57   perturbing firing rates in V1 through prolonged sensory deprivation results in a slow but

58   precise homeostatic regulation of firing back to an individual set-point, showing that

59   neurons actively maintain these set points over long time-scales (Hengen et al., 2016).

60   This stability in mean firing rates, even across periods of light and dark, raises the

61   question of how natural visual input is encoded by V1 activity in freely behaving

62   animals. One possibility is that changes in visual drive result in rapid fluctuations in

63   mean firing rates that operate over seconds to minutes. Another possibility is that firing

64   rates are stabilized even over these short time scales, and visual information is primarily

65   encoded in higher order network dynamics.

66   To generate insight into these questions we followed firing of individual neurons

67   in V1 of freely behaving young rats over several days, as animals experienced normal

68   light-dark (L-D) and dark-light (D-L) transitions, or transitions that were unexpectedly

69   imposed. We found that expected L-D transitions had a very modest effect on firing rates

70   of both excitatory and inhibitory neurons, even when examined immediately around the

71   time of the transition. Population activity did not change significantly across these

72   transitions, and when examined at the level of individual neurons only a small subset

73   (~15%) of excitatory neurons consistently responded, and then only during D-L

74   transitions when animals were awake. Interestingly, randomly timed transitions

75   throughout the light-dark cycle elicited more consistent responses across sleep-wake

76   states and at both D-L and L-D transitions, and robust and widespread responses to D-L

77   transitions could be unmasked by exposing animals to prolonged darkness for 60 hours.

78   These results suggest that the stability normally observed at expected (circadian) L-D

79   transitions reflects an active process of stabilization. Finally, although mean rates were

5

80   very similar in L and D, the pairwise correlations between simultaneously recorded

81   neurons were significantly higher in the light than in the dark, even when controlling for

82   behavioral state. Together our findings show that firing rates in V1 are actively stabilized

83   as animals navigate dramatic changes in the visual environment, and that the correlational

84   structure of V1 activity may carry more information about natural visual scenes than

85   firing rates.

86

Materials and Methods

All surgical and experimental procedures were approved by the Animal Care and Use Committee of Brandeis University and complied with the guidelines of the National Institutes of Health.

Surgery and in vivo *experiments*. The data analyzed in this study were collected in previous electrophysiological recordings (Hengen et al., 2016; n = 7 rats), as well as from newly implanted animals (n = 7 rats). All surgical procedures were as described previously (Hengen et al., 2013). Briefly, Long-Evans rats of either sex were bilaterally implanted with custom 16-channel 33 μm tungsten microelectrode arrays (Tucker-Davis Technologies, Alachua, FL) into monocular primary visual cortex (V1m) on postnatal day 21 (P21). Location was confirmed post-hoc via histological reconstruction. Two EMG wires were implanted deep in the nuchal muscle. Animals were allowed to recover for two full days post-surgery in transparent plastic cages with *ad libitum* access to food and water. Recording began on the third day after surgery. The recording chamber (a 12"x12" plexiglass cage with walls lined with high contrast low spatial frequency gratings) was lined with 1.5" of bedding and housed two rats. Animals had *ad libitum* food and water, and were separated by a clear plastic divider with 1" holes to allow for tactile and olfactory interaction while preventing jostling of headcaps and arrays. Electrodes were connected to commutators (TDT) to allow animals to freely behave throughout the recordings. Novel toys were introduced every 24h, to promote activity and exploration. Lighting and temperature were kept constant (LD 12:12, lights on at 7:30 am, 21° C, humidity 25%-55%). Data were collected continuously for nine to eleven days (200-240 hours). Some animals (n = 11 rats) underwent a lid suture and/or eye reopening

7

110   procedure on the third day of recording; in the present study we only analyzed data

111   collected from the control hemisphere ipsilateral to the manipulated eye. For dark-

112   exposure experiments, animals were kept in the dark starting on days 4 and 5 of the

113   recording (i.e. starting at the time of lights off on day 3, from P26 to P28). Lights came

114   on at the regular time (7:30 AM) on day 6 (P29).

115   *Electrophysiological recordings. In vivo* electrophysiological recordings were

116   performed as previously described (Hengen et al., 2016). Briefly, data were acquired at

117   25 kHz, digitized and streamed to disk for offline processing using a Tucker-Davis

118   Technologies Neurophysiology Workstation and Data Streamer. Spike extraction and

119   sorting was performed using custom MATLAB code. Spikes were detected as threshold

120   crossings (-4 s.d. from mean signal) and re-sampled at 3x the original rate. Each wire's

121   waveforms were then subjected to principal component analysis (PCA) and the first four

122   principal components were used for clustering using KlustaKwik (Harris et al., 2000).

123   Clusters were merged or trimmed as described previously (Hengen et al., 2016). Spike

124   sorting was done using custom MATLAB code relying on a random forest classifier

125   trained on a manually scored dataset of 1200 clusters. For each cluster identified from the

126   output of KlustaKwik, we extracted a set of 19 features, including ISI contamination (%

127   of ISIs < 3 ms), similarity to regular spiking unit (RSU) and fast-spiking (FS) waveform

128   templates, 60 Hz noise contamination, rise and decay time and slope of the mean

129   waveform, waveform amplitude and width. Cluster quality was also ensured by

130   thresholding of L-Ratio and Mahalanobis distance (Schmitzer-Torbert et al., 2005). The

131   random forest algorithm classified clusters as noise, multi-unit or single-unit. Only single

132   units with a clear refractory period were used for further analysis. Units were classified as

133   RSU or FS based on the time between the negative peak and the first subsequent positive

134   peak of the mean waveform (Fig. 1B). Clusters were classified as RSUs if this value was

135   > 0.39 msec, and as FS otherwise (Niell & Stryker, 2008), with a lower threshold of 0.19

136   msec to eliminate noise. We used previously established criteria and methods to select

137   neurons that we could reliably follow over time (Hengen et al., 2016); only neurons that

138   could be recorded for at least 48 consecutive hours were used for analysis of light-dark

139   transitions. For extended dark experiments, we analyzed all neurons that were online for

140   at least one hour preceding and one hour following the time of light re-exposure. For

141   estimates of mean firing during the extended dark phase, we analyzed the activity of all

142   cells that could be recorded in the first and last 12-hour period during the 60 hours of

143   darkness.

144   *Behavioral state classification.* The behavioral state of animals was classified using a

145   combination of local field potential (LFP), EMG and estimate of locomotion based on

146   video analysis (see Hengen et al., 2016). LFPs were extracted from three separate

147   recorded channels, resampled at 200 Hz, and averaged. The power spectral density was

148   computed in 10-second bins using a fast Fourier transform method (MATLAB

149   "spectrogram" function) using frequency steps of 0.1 Hz from 0.3 to 15 Hz. Power in the

150   delta (0.3 - 4 Hz) and theta (6 – 9 Hz) bands was computed as a fraction of total power in

151   each time bin. A custom algorithm was used to score each 10-second bin and assign one

152   of four behavioral codes, based on the power in each frequency band as well as EMG and

153   movement activity: active wake (high EMG and movement, low delta and theta), quiet

154   wake (low EMG and movement, low delta and theta), REM sleep (very low EMG, no

155   movement, low delta, high theta), and NREM sleep (low EMG and movement, high

9

156 delta, low theta). For each animal, each hour of data was scored separately. The first ten

157 hours were scored manually, and used as an initial training set for a random forest

158 classifier (implemented in Python). The classifier was then used to score each successive

159 hour, with manual corrections performed as needed. The classifier was re-trained after

160 every hour scored, with a maximum number of 10,000 bins used for training (only the

161 latest 10,000 bins were used).

162 *Extended darkness, immunostaining and image analysis.* For analysis of c-fos protein

163 following extended darkness, we transferred animals to custom dark box on P21. A light

164 timer was set up to allow for complete control of the light-dark cycle inside the box.

165 When animals were P26, lights were allowed to turn off at the regular time (7:30 PM),

166 and set up to not turn back on. Animals were in complete darkness for 60 hours, from the

167 night of P26 until night of P28 (ages matched with electrophysiological recordings). On

168 the morning of P29, lights were allowed to turn back on at 7:30 AM. Animals were

169 allowed to experience one hour of light before being deeply anesthetized and

170 transcardially perfused. Control animals were either not exposed to darkness but kept on

171 a regular 12h cycle, or anesthetized at 7:30 AM on P29 (before lights on) in the dark

172 using night-vision goggles and then immediately perfused. Brains were fixed in 3.7%

173 formaldehyde and 60 μm coronal slices of V1m were taken on a vibratome (Leica

174 VT1000S). Slices were immersed in a solution of PBS and NaN_3 and stored for

175 immunostaining. To ensure consistent results between groups, all conditions were run in

176 parallel. Slices were incubated for in a primary antibody solution (1:1000, Rabbit anti-c-

177 fos, Cell Signaling Technologies) at room temperature for 24 hours. They were then

178 rinsed and incubated for 2 hours with a secondary antibody (anti-rabbit Alexa Fluor 568,

10

179   1:400, Thermofisher). Sections were mounted on microscope slides with a DAPI-

180   containing medium (DAPI Fluoromount-G, Southern Biotech), coverslipped and allowed

181   to dry for 24 hours before imaging. Imaging was performed on a confocal microscope

182   (Zeiss Laser Scanning Microscope 880). A 10X objective was used to take z-stacks of

183   V1m in the DAPI and c-fos channels. Imaging settings were optimized for each

184   staining/imaging session and kept constant across conditions; all conditions were imaged

185   on a given session. Images were imported into Metamorph software for analysis. A

186   granularity analysis was used to determine locations of cell bodies, and co-localized

187   DAPI- and c-fos-positive granules were counted as c-fos-positive neurons. For each slice

188   we analyzed the whole field of view, excluding the slice edges as they displayed DAPI

189   staining artifacts.

190   *Analysis of electrophysiological data.* All electrophysiology data was analyzed using

191   a custom code package written in Python. The precise time of lights on/off was

192   determined by analysis of video recordings or using a light-sensitive resistor. All analyses

193   were performed on the 10 minutes before and after transitions. Peri-event time

194   histograms were obtained by binning data in 0.25 second bins and normalizing data to the

195   pre-transition period. Firing rates were estimated by sliding a 1 or 2 minute window in

196   20-second steps. Mean and s.e.m. were estimated by averaging across days. To compare

197   population data across transitions we calculated the average firing rate in the 10 minutes

198   before and after the transition without binning. For analysis restricted to a given

199   behavioral state, we only considered transitions during which the animal was in that state

200   for the whole 20 minutes (10 minutes before and after the transition). To estimate the

201   number of individual neurons that consistently changed their firing rate in response to L-

11

202   D and D-L transitions, we used a paired t-test to determine whether the neuron's firing

203   followed a consistent pattern of change across multiple transitions. We used a bootstrap

204   method to estimate the number of cells expected to pass our significance threshold by

205   chance; for each iteration of the bootstrap, we chose a random time point within the first

206   24h. We then created dummy transition times at 12 hour intervals from that starting time

207   point, and used these dummy transition points to repeat the above analysis for each cell.

208   This procedure was repeated 100 times (i.e. with 100 different dummy transition points),

209   to obtain 100 values for the percent of significantly changing cells. We used this dataset

210   to estimate the mean and 95% confidence intervals for this parameter. Only neurons that

211   were followed through at least 4 transitions were used for analysis of circadian

212   transitions. For non-circadian transitions, we analyzed neurons that experienced at least 6

213   transitions.

214   *Pairwise correlations.* Each spike train was binned into spike counts of bin size

215   100 ms, generating a vector of spike counts for each cell. The spike count correlation

216   coefficient ρ for a pair of neurons was computed in 30 minute episodes using a

217   sliding window of 5 minutes. This produced 139 values for each neuron pair on

218   every single half day (12 hours of light and 12 hours of darkness). The average of

219   these values then determined the correlation value of each pair for every single half

220   day:

$$\rho_{X,Y} = \frac{E[(X - \mu_X)(Y - \mu_Y)]}{\sigma_X \sigma_Y}$$

221

222   where X and Y represent the spike count vectors of two cells, respectively; μ_X and μ_Y

223   are the means of X and Y; σ_X and σ_Y denote the standard deviations of X and Y; E is the

12

224 expectation. This produced the matrices of pairwise spike count correlations on different

225 half days. To generate the normalized correlation curve, correlations were normalized to

226 the average correlation of each animal at P26 during the light period. Correlations in

227 mixed behavioral states were computed with the above-stated method using the entire 12-

228 hour periods of L or D, while correlations in wake only took into account the wake

229 episodes. Results with bin size of 5 ms followed the same approach.

230 *Experimental design and statistical analysis*. For paired data, both for firing rates and

231 spike count correlations, comparisons were done using a Wilcoxon signed-rank test. To

232 compare a population mean to a given value (e.g. 0) we used one-sample t-tests. To

233 compare cumulative distributions we used Kolmogorov-Smirnov tests. Data are

234 represented as mean ± s.e.m. Box plots represent median ± interquartile range, with

235 whiskers extending to the rest of the distribution. All statistical analyses were performed

236 using Python.

237 *Code accessibility*. All code used for analysis is available from the authors upon

238 request.

239

13

240

Results

242   Neurons in V1 maintain remarkably similar mean firing rates in L and D, but how

243   L-D transitions affect firing on more rapid time scales in freely viewing and behaving

244   animals is unclear. Here we use chronic *in vivo* electrophysiological recordings from

245   freely behaving rats to closely examine the activity of V1 neurons at D-L and L-D

246   transitions in regular (12h/12h) and manipulated light/dark cycles, and during unexpected

247   light-dark transitions. Using previously established methods (Hengen et al., 2016) we

248   followed individual neurons over time and across multiple light transitions. This

249   approach allowed us to analyze the dynamics of neuronal activity at different timescales

250   in response to the appearance or disappearance of natural visual stimuli.

251

The appearance or disappearance of natural visual stimuli has only a modest effect on the mean firing rates of V1 neurons.

254   The firing rates of V1 neurons recorded in freely behaving young rats in light and

255   dark are exceedingly similar when averaged in 12-hour periods (Hengen et al., 2016).

256   Here we combine previously and newly acquired datasets and set out to re-analyze the

257   activity of V1 neurons around the transition from presence to absence of visual input

258   (light-dark, L-D), and vice versa (dark-light, D-L) (Fig. 1A). Recorded neurons were

259   classified as regular spiking units (RSU, n = 96) or fast-spiking cells (FS, n = 32) based

260   on waveform shape and according to established criteria (Fig. 1B; Niell & Stryker, 2008;

261   Hengen et al., 2013). These populations are mostly comprised of excitatory pyramidal

14

262   neurons (RSU) and GABAergic parvalbumin-containing interneurons (FS) (Kawaguchi

263   & Kubota, 1993; Nowak et al., 2003).

264   As rats experience L-D or D-L transitions, most neurons showed little change in

265   firing (Fig. 1C). We treated each transition as a separate trial and estimated the firing rate

266   for each cell as the average of the peri-event time histogram (PETH) centered on the

267   transition. We first aimed to compare activity at the population level in different stimulus

268   conditions. To this end, we determined whether the distributions of mean firing rates

269   averaged over 10 minutes on either side of the L-D and D-L transitions were similar to

270   each other. Cumulative distributions in light and dark were indistinguishable, for both

271   RSU and FS cells, in all conditions (Fig. 1D, E; two-sample Kolmogorov-Smirnov test,

272   RSU, L-D: $p = 0.88$; D-L: $p = 0.99$; FS, L-D: $p = 0.99$; D-L: $p = 1.0$). Similarly, when we

273   compared the distributions using a Wilcoxon rank-sum test, we found no difference

274   between the distributions of mean firing rates before vs. after the transitions (Wilcoxon

275   rank-sum test, RSU, L-D: $p = 0.677$; D-L: $p = 0.655$; FS, L-D: $p = 0.905$; D-L: $p =$

276   0.827).

277   Next we took advantage of our ability to follow individual neurons across

278   transitions to examine the data in a paired manner, where the firing rate of each neuron

279   was compared before and after the transition. For each neuron we computed mean firing

280   rate in the 10 minutes before and after the transition time, and averaged across transitions

281   of the same type to estimate the average effect on individual neuronal firing. This

282   analysis revealed a small but consistent change in mean RSU firing rates across both L-D

283   and D-L transitions (Fig. 1F; Wilcoxon sign-rank test: L-D: $p = 0.0002$; D-L: $p <$

284   0.0001), while the activity of FS cells only changed significantly at D-L transitions (Fig.

15

285   1G; Wilcoxon sign-rank test: L-D: p = 0.318; D-L: p = 0.026). The magnitude of these

286   effects was small, on order 7-15% for RSUs (Fig. 1H, I; RSU, L-D: -7.09% ± 1.99%, p =

287   0.0006; D-L: 15.60% ± 4.00%, p = 0.0002; FS, L-D: -2.75% ± 3.80%, p = 0.475; D-L:

288   9.73% ± 5.12%, p = 0.067, one-sample t-test).

289   These data show that, surprisingly, dramatic changes in visual input cause very

290   minor changes in V1 firing rates. The distributions of mean rates in the presence and

291   absence of natural visual stimuli are identical in the proximity of transitions. Analysis of

292   many transitions shows that RSU firing rates are consistently affected when the visual

293   environment changes, but this modulation is decidedly modest.

294

295   **Behavioral state affects sensitivity of firing rates to visual stimuli**

296   As rats were freely behaving throughout all experiments, we considered whether

297   their alertness state at the light transitions could affect the activity of V1 neurons. LFP,

298   EMG and video data were collected and used to score animals' behavioral state into

299   either asleep or awake (Hengen et al., 2016). For each animal, 20-minute periods

300   centered on the L-D and D-L transitions were considered. Only periods during which the

301   animal remained in the same behavioral state for the entire time were analyzed. For each

302   neuron, we plotted the mean firing rate before the transition against the mean rate after

303   the transition. The activity of neurons proved to be strikingly similar across all

304   transitions, whether the animals were awake or asleep (Fig. 2A, B). In either behavioral

305   state, firing rates in light and dark were very strongly correlated, and the slope of the

306   regression line was close to one (RSU, wake, L-D: slope = 0.959, r = 0.966, p < 10^{-43}; D-

307   L: slope = 0.960, r = 0.991, p < 10^{-48}; FS, wake, L-D: slope = 1.113, r = 0.964, p < 10^{-13};

16

308   D-L: slope = 0.976, r = 0.990, p < 10^{-18}; RSU, sleep, L-D: slope = 1.147, r = 0.941, p <

309   10^{-12}; D-L: slope = 0.990, r = 0.996, p < 10^{-13}; FS, sleep, L-D: slope = 1.093, r = 0.987, p

310   < 10^{-13}; D-L: slope = 1.003, r = 0.996, p < 10^{-11}).

311   We again looked at the data in paired form, by comparing a neuron's average

312   firing rate on either side of a L-D transition. The mean activity of RSUs in V1 changed

313   consistently across transitions when animals were awake (Fig. 2C; L-D: p = 0.0001; D-L:

314   p = 0.0457, Wilcoxon signed-rank test), but not when they were asleep (Fig. 2D; L-D: p

315   = 0.656; D-L: p = 0.925, Wilcoxon signed-rank test). We observed a similar pattern in FS

316   cells, although the data in the wake condition was not significant for light-dark transitions

317   (Fig. 2E, F; Wake, L-D: p = 0.689; D-L: p = 0.039; Sleep, L-D: 0.557; D-L: p = 0.638;

318   Wilcoxon signed-rank test). Once again, these effects were of small magnitude (7-12%).

319   Thus, V1 neurons do not respond to expected (circadian) changes in the visual

320   environment when animals are asleep, and respond only modestly when animals are

321   awake.

322

323   **A sub-population of RSUs is consistently responsive to dark-light transitions**

324   While we only detected small changes at the population levels (and no change in

325   the population distribution), we occasionally observed neurons whose activity appeared

326   to be consistently modulated by visual stimuli. The majority of neurons showed no

327   spiking modulation across multiple transitions (Fig. 3A), but a subset of neurons showed

328   higher activity on one side of the transition (Fig. 3B). Occasionally neurons responded to

329   both L-D and D-L transitions (Fig. 3B), but more often neurons were only responsive to

330   one or the other. To quantify these observations, we treated each transition independently

17

331 for each neuron, and averaged firing rates for 10 minutes before and after lights on/off,

332 and identified neurons that changed their firing rate consistently across transitions using a

333 paired t-test.

334   Because neuronal firing rates are variable, we presumed that some of these

335 apparent responses were spurious. To estimate the false positive rate we performed a

336 bootstrap analysis using random time points as dummy "transitions". We chose nine

337 transition points 24 hours apart from each other (to match circadian transitions) and

338 analyzed mean firing rates for each neuron as above but using these dummy transition

339 points. This process was repeated 100 times to arrive at an estimate of the mean and 95%

340 confidence interval for the percentage of responsive cells (mean and 95% CI, RSU, L-D:

341 3.55% [0% - 12.62%], D-L: 3.09% [0% - 9.91%]; n= 64).

342   The proportion of cells we found to be transition-responsive was within the range

343 expected by chance for all conditions except for RSUs in D-L transitions (Fig. 3C). We

344 found that 14% of RSUs in our experimental condition had significantly changing firing

345 rates from dark to light, well outside the range expected by chance (95% CI for this

346 group: [0% - 9.91%]). In addition, most of these neurons (88.9%) showed an increase in

347 firing rate at the onset of light, while in the bootstrap control neurons were found to have

348 an equal probability of increasing or decreasing their activity at a given transition point

349 (51.8% of neurons increasing).

350   Finally, we examined the temporal dynamics of firing rate changes for the subset

351 of RSUs that were consistently responsive to D-L transitions. We plotted the mean

352 activity within 1 hour of the transition, across all transitions and across neurons for this

353 subpopulation (Fig. 3D). On average, the change in FR was short-lived, on the order of

18

354   ~10 minutes, and of moderate size (~25% increase). This analysis shows that a small

355   subset of excitatory pyramidal neurons in V1 consistently modulate their activity in

356   response to the expected appearance of visual input after a circadian 12-hour period of

357   darkness. This change is transient, with firing rates returning to pre-transition levels

358   within minutes.

359

360   **Light transitions have no effect on average ISIs over short timescales**

361   Our analysis so far shows that, on a timescale of 10s of minutes, few V1 neurons

362   show significant firing rate modulation to the appearance or disappearance of natural

363   visual stimuli. One possible explanation for this apparent lack of responsiveness is that

364   these dramatic sensory changes trigger a rapid adaptation mechanism that quickly

365   restores average V1 activity back to baseline. Such adaptation mechanisms within V1

366   have been well described, and can operate on a time-scale of 100s of ms to many minutes

367   (Kohn, 2007; Wissig and Kohn, 2012; Benucci et al., 2013). To address this possibility,

368   we examined neuronal firing in 1-, 10- and 30-second intervals around L-D and D-L

369   transitions. Spiking in these short time windows was sparse and variable across days (Fig.

370   4A, B). We averaged the mean inter-spike interval (ISI) across days for each cell, and

371   compared averages in the 10 seconds before and after transitions. To ensure we were not

372   missing effects on even shorter timeframes we also computed the mean ISI in 1-second

373   windows around the transitions. For both the 1-sec and the 10-sec case, we found no

374   statistically significant effect (Fig. 4C, 1-sec, L-D: $p = 0.27$; D-L: $p = 0.36$; Fig. 4D, 10-

375   sec, L-D: $p = 0.97$; D-L: $p = 0.31$; Wilcoxon sign-rank test). Similar results were obtained

376   when this analysis was carried out with 5-sec and 30-sec intervals (data not shown). This

19

377   indicates that the stability of firing across transitions is not due to a short-term adaptation

378   process that rapidly restores firing to baseline.

379

380   **Non-circadian, unexpected L-D transitions are more likely to perturb V1 firing**

381   **rates**

382   All of our data so far suggest that dramatic changes in visual input at circadian L-

383   D transitions have very subtle effects on V1 firing. We wondered if this might be due to

384   circadian entrainment, i.e. that when L-D and D-L transitions happen at regular times

385   they are expected and the response of neurons to otherwise salient stimuli is attenuated.

386   To test this, we examined neuronal responses to stimulus transitions occurring at random

387   points in the circadian cycle.

388   We recorded single-unit activity in V1 while turning the lights off (or on) for 10

389   minutes during the light (or dark) cycle (Fig. 5A, n = 6 animals). We then calculated the

390   number of neurons that consistently and significantly changed their firing at these

391   unexpected transitions, and again used a bootstrap analysis to calculate the false positive

392   rate. In marked contrast to expected transitions (Fig. 3D), we found that both L-D and D-

393   L unexpected transitions caused a subset of RSUs to consistently modulate their spiking

394   (Fig. 5B, C). This effect was seen regardless of behavioral state (significantly changing

395   RSUs, sleep, L-D: 21.9%, n = 64; D-L: 13.4%, n = 67; wake, L-D: 17.6%, n = 91; D-L:

396   12.7%, n = 55) and the proportion of significantly changing neurons was higher than

397   expected by chance in most conditions (bootstrap mean and 95% CI, RSU, sleep, L-D:

398   4.42% [0% - 8.95%], D-L: 4.31% [0% - 9.38%]; RSU, wake, L-D: 4.22% [0% - 8.79%],

399   D-L: 4.33% [0% - 9.09%]).

20

400   These results show that more neurons respond consistently to L-D and D-L

401   transitions when these do not line up with the circadian cycle the animals are entrained

402   on. However, even during unexpected transitions only a minority (12%-20%) of neurons

403   consistently changed their firing rate in response to the appearance or disappearance of

404   natural visual stimuli.

405

406   **Pairwise correlations in V1 are significantly higher in light than in dark**

407   To investigate whether higher order network properties are modified by the

408   presence or absence of natural visual stimuli, we examined the structure of pairwise

409   correlations in light and in dark (Fig. 6, n = 5 animals). Plotting the correlation matrices

410   of one animal at P27 revealed that these correlations were higher in the light (calculated

411   over the 12-hour period at P27) than in the dark (calculated over the 12-hour period at

412   P27.5; Fig. 6A). We then plotted the average correlation computed continuously over 4

413   days (normalized to the average correlation of each animal at P26 in light) (Fig. 6B). The

414   normalized pairwise correlation showed a pronounced oscillation across light and dark

415   periods, and was consistently higher in the light. To assess the degree to which

416   correlation of individual pairs changed, we compared the correlation of 922 pairs in light

417   versus dark computed for spike counts with bin sizes of 5 or 100 ms, respectively. We

418   found that correlations in light were higher than in dark for both bin sizes (Fig. 6C; left, 5

419   ms: $p < 10^{-70}$; right, 100 ms: $p < 10^{-125}$, Wilcoxon signed-rank test). To ensure that the

420   observed difference of correlations between light and dark was not caused by

421   disproportionate time spent in wake or sleep, we restricted the analysis to periods of

422   wake, and again computed the average correlation. Consistent with our previous analysis,

21

423   correlations in wake during light were significantly greater than in wake during dark (Fig.

424   6D; left, 5 ms: $p < 10^{-55}$; right, 100 ms: $p < 10^{-110}$, Wilcoxon signed-rank test). These

425   results indicate that the presence of natural visual stimuli increases pairwise correlations

426   in V1.

427

428   **Prolonged dark exposure enhances the responsiveness of V1 neurons to natural**

429   **visual input**

430   Our data show that re-exposure to light after 12 h of darkness has only modest

431   effects on V1 firing; in contrast, re-exposing animals to light after a period of *prolonged*

432   darkness is a standard paradigm for increasing activity-dependent gene expression in V1

433   (Rosen et al., 1992; Mower, 1994; Kaminska et al., 1996; reviewed in Kaczmarek and

434   Chaudhuri, 1997). We therefore wondered whether prolonged dark exposure might

435   unmask robust responses to the sudden onset of visual stimuli within V1.

436   We began by using expression of the immediate early gene *c-fos*, which is driven

437   by enhanced calcium influx during elevated activity (Bartel et al., 1989; Sheng et al.,

438   1990; reviewed in Sheng and Greenberg, 1990). After prolonged darkness, brief light

439   exposure induces widespread *c-fos* expression in V1 of cats and rodents (Rosen et al.,

440   1992; Kaplan et al., 1996; Yamada et al., 1999; Mower and Kaplan, 2002). To replicate

441   this we placed P26 rats in the darkness for 60 hours (12 hours + 2 days) and then exposed

442   them to light for one hour before immunostaining for the c-fos protein (light exposed, n =

443   28 slices, 5 animals). We used age-matched animals either exposed to one hour of light

444   after a regular 12h/12h cycle (regular control, n = 22 slices, 4 animals), or kept in the

445   dark for 60 hours but sacrificed before lights on (dark control, n = 23 slices, 4 animals),

446 as controls (Fig. 7A, B). Animals in the light exposure condition showed an elevated

447 percentage of c-fos-positive cells (Fig. 7C; RC: 11.4% ± 1.6%; DC: 6.1% ± 0.8%; LE:

448 16.8% ± 1.7%. LE vs RC p=0.032; LE vs DC p=0.001, one-way ANOVA with Tukey

449 post-hoc test), as well as increased total staining intensity (Fig. 7D; normalized to RC,

450 RC: 1.00 ± 0.06; DC: 0.79 ± 0.05; LE: 1.31 ± 0.09. LE vs RC p=0.011; LE vs DC

451 p=0.001, one-way ANOVA with Tukey post-hoc test). These data confirm that a 60-hour

452 period of prolonged darkness is sufficient to induce increased expression of *c-fos* in

453 rodent V1.

454 Next we asked whether this elevated *c-fos* expression was correlated with

455 increased firing. We used the same paradigm as above but recorded continuously from

456 V1 during the baseline, dark-exposure, and light re-exposure period (n = 4 animals).

457 Upon light re-exposure, both RSUs and FS cells showed a substantial transient increase

458 in firing rate at the time of lights on (Fig 8A; RSU: n = 32; FS: n = 12). We compared

459 average firing rates 10 minutes before and after the transition for each cell. Both FS and

460 RSU populations showed a significant increase in firing rate following light exposure

461 (Fig. 8C, D; RSU: $p < 10^{-5}$; FS: $p = 0.034$; Wilcoxon signed-rank test). The percent

462 change in firing rate across the transition was also significantly different from zero (Fig.

463 8B; all cells: 87.1% ± 13.5%, $p < 10^{-7}$; RSU: 80.7% ± 14.9%, $p < 10^{-5}$; FS: 104.3% ±

464 29.8%, p = 0.005; one-sample t-test), and the majority of neurons increased their activity

465 at lights on (RSU: 31/32 neurons; FS: 10/12 neurons).

466 It has been reported that prolonged dark exposure increases firing rates in rodent

467 V1 (Bridi, de Pasquale, Lantz et al., 2018), suggesting that enhanced responsiveness to

468 light re-exposure might arise from increased excitability of V1 circuitry. To examine this

469   we asked how prolonged dark exposure affected RSU firing rates in freely behaving

470   animals prior to light re-exposure. When we compared the distribution of RSU firing

471   rates during the first and last 12 hours of the 60-hour long period of prolonged darkness,

472   rather than an increase, we found a small but significant *decrease* in firing rates (Fig. 8E;

473   mean ± s.e.m, first 12h: 4.00 ± 0.97 Hz, last 12h: 2.27 ± 0.57 Hz; median, first 12h: 1.18

474   Hz; last 12h: 0.85 Hz; p = 0.044, Wilcoxon rank-sum test). Thus the enhanced

475   responsiveness to restoration of natural visual stimuli is unlikely to be due to a simple

476   global increase in circuit excitability. These data indicate that prolonged dark exposure

477   disrupts the normal stability of V1 firing across D-L transitions, and suggests that the

478   maintenance of this stability is dependent upon visual experience.

479

Discussion

How internal and external factors influence the long-term dynamics of neuronal firing in V1 is poorly understood. Here we recorded from ensembles of single units over a period of several days in freely viewing and behaving animals and found that firing rates of both excitatory and inhibitory V1 neurons were remarkably stable even when sensory input changed abruptly and dramatically. During expected circadian L-D transitions very few V1 neurons significantly changed their firing. A larger subset of V1 neurons were consistently responsive to unexpected L-D transitions, and disruption of the regular L-D cycle with two days of complete darkness induced a widespread and robust increase in V1 firing upon subsequent re-introduction of visual input. These data show that V1 neurons fire at similar rates in the presence or absence of natural visual stimuli, and that significant changes in mean activity arise only in response to unexpected changes in the visual environment. While mean firing rates were not different in L and D, pairwise correlations were significantly stronger in the light in the presence of natural visual stimuli, suggesting that information about natural scenes in V1 is more readily extractable from pairwise correlations than from individual firing rates. Taken together, our findings are consistent with a process of rapid and active stabilization of firing rates during expected changes in visual input, and demonstrate that firing rates in V1 are remarkably stable at both short and long timescales.

The near absence of firing rate modulation in response to the appearance (or disappearance) of natural visual stimuli may seem surprising, as there is a rich literature supporting the idea that V1 neurons respond to optimal stimuli by

25

503   increasing their spiking (Hubel and Wiesel, 1959, 1962; Campbell et al., 1968;

504   Pettigrew, 1974; Henry et al., 1974; Movshon, 1975; De Valois et al., 1982; Gizzi et

505   al., 1990; Carandini and Ferster, 2000). Many of these studies used anesthetized

506   preparations, making comparisons with our results difficult, but our data are

507   consistent with previous reports of small differences in overall activity between

508   natural vision and complete darkness in awake animals (Fiser et al., 2004), and

509   sparse modulation of spiking in response to natural scene viewing (Gallant et al.,

510   1998; Vinje and Gallant, 2000; Haider et al., 2010; Herikstad et al., 2011). In general

511   our data support the view that mean firing rates in V1 can be stabilized over both

512   long (Hengen et al., 2016) and short timescales without interfering with visual

513   coding, which may arise through very sparse modulation of spiking and/or higher

514   order population dynamics (Haider et al., 2010; Vinck et al., 2015; Dipoppa et al.,

515   2018).

516   Despite the lack of robust changes in population spike rates at D-L

517   transitions, we did observe a small subset of neurons that transiently increased

518   their firing specifically at the appearance of visual input (Fig. 4). Since this occurred

519   in freely behaving animals, it is unlikely that these neurons were responding to the

520   same optimal visual stimuli on consecutive days. The more parsimonious

521   explanation seems to be that these are broadly tuned neurons that become activated

522   at most D-L transitions. Interestingly, we detected a greater proportion of such

523   transition-responsive cells when light transitions happened randomly throughout

524   the L-D cycle, including a population of neurons that transiently responded to non-

525   circadian L-D transitions by decreasing their firing rate (Fig. 4). Thus unexpected

26

526 changes in visual drive unmask robust and bidirectional changes in firing in a small

527 subset (15-20%) of V1 neurons. There are several potential explanations for this

528 effect. It is possible that the responsive neurons are specialized to represent this

529 "unexpectedness" as an error signal, as has been proposed in some models of

530 predictive coding (Rao and Ballard, 1999; Egner et al., 2010). Alternatively, it could

531 be the result of modulation by other brain areas that encode the surprise signal,

532 akin to that seen in response to attention or reward cues (Shuler and Bear, 2006;

533 Stănişor et al., 2013), or during modulation of V1 by locomotion (Niell and Stryker,

534 2010). Finally, our data cannot distinguish between this last possibility and the

535 opposite signal, i.e. a suppression of responses at expected transitions.

536   We were able to disrupt the normal conservation of firing rates across D-L

537 transitions even more dramatically by using a prolonged dark-exposure paradigm,

538 which induced a network-wide enhancement of firing upon light re-exposure. This

539 paradigm is thought to induce metaplastic changes within V1 that increase AMPA

540 quantal amplitude onto L2/3 pyramidal neurons (Goel and Lee, 2007; Blackman et

541 al., 2012; Bridi, de Pasquale, Lantz et al., 2018), but the impact of these changes on

542 overall V1 function and excitation/inhibition balance are unclear. A previous study

543 in anesthetized animals found that several days of dark exposure increased firing

544 rates in V1, raising the possibility that prolonged dark exposure increases overall V1

545 excitability (Bridi, de Pasquale, Lantz et al., 2018); however, here we found a small

546 but significant reduction in mean firing rate across the population in freely behaving

547 animals, suggesting that circuit excitability is if anything reduced by prolonged dark

548 exposure. Although the circuit mechanism by which dark exposure unmasks robust

27

549 responses to D-L transitions is unclear, these experiments suggest that normal

550 visual experience is necessary to maintain the ability of V1 circuits to stabilize their

551 firing across these transitions.

552 In contrast to our observations on the stability of firing rates, we found that

553 pairwise correlations in visual cortex were markedly higher in the light phase than

554 in the dark phase (Fig. 5). This is consistent with previous reports that ongoing

555 spontaneous activity in the dark is less correlated than activity elicited by natural

556 scene stimuli (Fiser et al., 2004; Karimipanah et al., 2017). Correlations are

557 dependent on the degree of synchrony within neuronal circuits (Harris and Thiele,

558 2011; Schölvinck et al., 2015) and are higher during anesthesia (Greenberg et al.,

559 2008), raising the possibility that this is a simple reflection of time spent in different

560 behavioral states during the L and D phase. However, we observed the same

561 increased correlation in L when only analyzing periods when animals were awake,

562 ruling out this possibility. Thus, we conclude that, in freely behaving and viewing

563 animals, sensory input can shift visual cortical circuits to more correlated dynamical

564 states, even in a condition of low synchrony when animals are awake.

565 Our results add to a growing body of work suggesting that ongoing activity in

566 mammalian V1 plays an important role in modulating sensory responses, as well as

567 in integrating other sensory, motor, and motivational signals (Tsodyks et al., 1999;

568 Rao and Ballard, 1999; Treue, 2001; Fiser et al., 2004; Luczak et al., 2009, 2013;

569 Goard and Dan, 2009; Ringach, 2009; Egner et al., 2010; Niell and Stryker, 2010;

570 Destexhe, 2011; Keller et al., 2012; Ayaz et al., 2013; Saleem et al., 2013; Vinck et al.,

571 2015). Our results also show that firing rates of most V1 neurons are remarkably

28

572   stable over both long and short time scales and in the presence and absence of

573   visual information, suggesting that most visual information during natural viewing

574   is not encoded by changes in firing rates. Instead, our data suggest that

575   perturbations in firing primarily occur during unexpected changes in visual input,

576   indicating an effect of entrainment/expectation and the existence of an active

577   mechanism for stabilization of activity. This may be of particular importance given

578   the observation that pairwise correlations are increased when animals are exposed

579   to visual input, as global fluctuations in firing rate can strongly affect the strength of

580   correlations between pairs of neurons (Harris and Thiele, 2011). Thus, it is possible

581   that stable firing rates enable changes in correlations to reflect differences in

582   sensory input, and hence to promote effective sensory processing.

583 **References**

584 Arieli A, Shoham D, Hildesheim R, Grinvald A (1995). Coherent spatiotemporal patterns

585   of ongoing activity revealed by real-time optical imaging coupled with single-unit

586   recording in the cat visual cortex. *Journal of neurophysiology*, *73*(5), 2072-2093.

587

588 Averbeck BB, Latham PE, Pouget A (2006). Neural correlations, population coding and

589   computation. *Nature reviews neuroscience*, *7*(5), 358-366.

590

591 Ayaz A, Saleem AB, Schölvinck ML, Carandini, M (2013). Locomotion controls spatial

592   integration in mouse visual cortex. *Current Biology*, *23*(10), 890-894.

593

594 Bartel DP, Sheng M, Lau LF, Greenberg ME (1989). Growth factors and membrane

595   depolarization activate distinct programs of early response gene expression:

596   dissociation of fos and jun induction. *Genes development*, *3*(3), 304-313.

597

598 Benucci A, Saleem AB, Carandini M (2013). Adaptation maintains population

599   homeostasis in primary visual cortex. *Nature neuroscience*, *16*(6), 724-729.

600

601 Blackman MP, Djukic B, Nelson SB, Turrigiano GG (2012). A critical and cell-

602   autonomous role for MeCP2 in synaptic scaling up. *Journal of*

603   *Neuroscience*, *32*(39), 13529-13536.

604

605   Bridi MCD, de Pasquale R, Lantz CL, Gu Y, Borrell A, Choi SY, He K, Lee HK,

606   Quinlan EM, Kirkwood A (2018). Two distinct mechanisms for experience-

607   dependent homeostasis. *Nature neuroscience*, 21, 843-850.

608

609   Campbell FW, Cleland BG, Cooper GF, Enroth-Cugell C (1968). The angular selectivity

610   of visual cortical cells to moving gratings. *The Journal of Physiology*, *198*(1),

611   237-250.

612

613   Carandini M, Ferster D (2000). Membrane potential and firing rate in cat primary visual

614   cortex. *Journal of Neuroscience*, *20*(1), 470-484.

615

616   Ch'Ng YH, Reid C (2010). Cellular imaging of visual cortex reveals the spatial and

617   functional organization of spontaneous activity. *Frontiers in integrative*

618   *neuroscience*, *4*, 20.

619

620   De Valois RL, Yund EW, Hepler N (1982). The orientation and direction selectivity of

621   cells in macaque visual cortex. *Vision research*, *22*(5), 531-544.

622

623   Destexhe A (2011). Intracellular and computational evidence for a dominant role of

624   internal network activity in cortical computations. *Current opinion in*

625   *neurobiology*, *21*(5), 717-725.

626

627   Dhawale AK, Poddar R, Wolff SB, Normand VA, Kopelowitz E, Ölveczky BP (2017).

628   Automated long-term recording and analysis of neural activity in behaving

629   animals. *Elife*, *6*, e27702.

630

631   Dipoppa M, Ranson A, Krumin M, Pachitariu M, Carandini M, Harris KD (2018). Vision

632   and locomotion shape the interactions between neuron types in mouse visual

633   cortex. *Neuron*, *98*(3), 602-615.

634

635   Egner T, Monti JM, Summerfield C (2010). Expectation and surprise determine neural

636   population responses in the ventral visual stream. *Journal of*

637   *Neuroscience*, *30*(49), 16601-16608.

638

639   Fiser J, Chiu C, Weliky M (2004). Small modulation of ongoing cortical dynamics by

640   sensory input during natural vision. *Nature*, *431*(7008), 573-578.

641

642   Gallant JL, Connor CE, Van Essen DC (1998). Neural activity in areas V1, V2 and V4

643   during free viewing of natural scenes compared to controlled

644   viewing. *Neuroreport*, *9*(1), 85-89.

645

646   Gizzi MS, Katz E, Schumer RA, Movshon JA (1990). Selectivity for orientation and

647   direction of motion of single neurons in cat striate and extrastriate visual

648   cortex. *Journal of neurophysiology*, *63*(6), 1529-1543.

649

650   Goard M, Dan Y (2009). Basal forebrain activation enhances cortical coding of natural

651   scenes. *Nature neuroscience*, *12*(11), 1444-1449.

652

653   Goel A, Lee HK (2007). Persistence of experience-induced homeostatic synaptic

654   plasticity through adulthood in superficial layers of mouse visual cortex. *Journal*

655   *of Neuroscience*, *27*(25), 6692-6700.

656

657   Greenberg DS, Houweling AR, Kerr JN (2008). Population imaging of ongoing neuronal

658   activity in the visual cortex of awake rats. *Nature neuroscience*, *11*(7), 749-751.

659

660   Haider B, Krause MR, Duque A, Yu Y, Touryan J, Mazer JA, McCormick DA (2010).

661   Synaptic and network mechanisms of sparse and reliable visual cortical activity

662   during nonclassical receptive field stimulation. *Neuron*, *65*(1), 107-121.

663

664   Harris KD, Henze DA, Csicsvari J, Hirase H, Buzsaki G (2000). Accuracy of tetrode

665   spike separation as determined by simultaneous intracellular and extracellular

666   measurements. *Journal of neurophysiology*, *84*(1), 401-414.

667

668   Harris KD, Thiele A (2011). Cortical state and attention. *Nature reviews*

669   *neuroscience*, *12*(9), 509-523.

670

671   Hengen KB, Lambo ME, Van Hooser SD, Katz DB, Turrigiano GG (2013). Firing rate

672   homeostasis in visual cortex of freely behaving rodents. *Neuron*, *80*(2), 335-342.

673

674 Hengen KB, Torrado Pacheco A, McGregor JN, Van Hooser SD, Turrigiano GG (2016).

675   Neuronal firing rate homeostasis is inhibited by sleep and promoted by

676   wake. *Cell*, *165*(1), 180-191.

677

678 Henry GH, Dreher B, Bishop PO (1974). Orientation specificity of cells in cat striate

679   cortex. *Journal of Neurophysiology*, *37*(6), 1394-1409.

680

681 Herikstad R, Baker J, Lachaux JP, Gray CM, Yen SC (2011). Natural movies evoke spike

682   trains with low spike time variability in cat primary visual cortex. *Journal of*

683   *Neuroscience*, *31*(44), 15844-15860.

684

685 Hubel DH, Wiesel TN (1959). Receptive fields of single neurones in the cat's striate

686   cortex. *The Journal of physiology*, *148*(3), 574-591.

687

688 Hubel DH, Wiesel TN (1962). Receptive fields, binocular interaction and functional

689   architecture in the cat's visual cortex. *The Journal of physiology*, *160*(1), 106-154.

690

691 Kaczmarek L, Chaudhuri A (1997). Sensory regulation of immediate–early gene

692   expression in mammalian visual cortex: implications for functional mapping and

693   neural plasticity. *Brain Research Reviews*, *23*(3), 237-256.

694

695   Kaminska B, Kaczmarek L, Chaudhuri A (1996). Visual Stimulation Regulates the
696   Expression of Transcription Factors and Modulates the Composition of AP-1 in
697   Visual Cortex. *Journal of Neuroscience*, *16*(12), 3968-3978.

698

699   Kaplan IV, Guo Y, Mower GD (1996). Immediate early gene expression in cat visual
700   cortex during and after the critical period: differences between EGR-1 and Fos
701   proteins. *Molecular brain research*, *36*(1), 12-22.

702

703   Karimipanah Y, Ma Z, Miller JEK, Yuste R, Wessel R (2017). Neocortical activity is
704   stimulus-and scale-invariant. *PloS one*, *12*(5), e0177396.

705

706   Kawaguchi Y, Kubota Y (1993). Correlation of physiological subgroupings of
707   nonpyramidal cells with parvalbumin-and calbindinD28k-immunoreactive
708   neurons in layer V of rat frontal cortex. *Journal of neurophysiology*, *70*(1), 387-
709   396.

710

711   Keck T, Keller GB, Jacobsen RI, Eysel UT, Bonhoeffer T, Hübener M (2013). Synaptic
712   scaling and homeostatic plasticity in the mouse visual cortex in
713   vivo. *Neuron*, *80*(2), 327-334.

714

715   Keller GB, Bonhoeffer T, Hübener M (2012). Sensorimotor mismatch signals in primary
716   visual cortex of the behaving mouse. *Neuron*, *74*(5), 809-815.

717

718   Kenet T, Bibitchkov D, Tsodyks M, Grinvald A, Arieli A (2003). Spontaneously
719   emerging cortical representations of visual attributes. *Nature*, *425*(6961), 954-
720   956.

721

722   Kohn A (2007). Visual adaptation: physiology, mechanisms, and functional
723   benefits. *Journal of neurophysiology*, *97*(5), 3155-3164.

724

725   Luczak A, Barthó P, Harris KD (2009). Spontaneous events outline the realm of possible
726   sensory responses in neocortical populations. *Neuron*, *62*(3), 413-425.

727

728   Luczak A, Barthó P, Harris KD (2013). Gating of sensory input by spontaneous cortical
729   activity. *Journal of Neuroscience*, *33*(4), 1684-1695.

730

731   MacLean JN, Watson BO, Aaron GB, Yuste R (2005). Internal dynamics determine the
732   cortical response to thalamic stimulation. *Neuron*, *48*(5), 811-823.

733

734   Miller KD, MacKay DJ (1994). The role of constraints in Hebbian learning. *Neural
735   Computation*, *6*(1), 100-126.

736

737   Movshon JA (1975). The velocity tuning of single units in cat striate cortex. *The Journal
738   of Physiology*, *249*(3), 445-468.

739

740   Mower GD (1994). Differences in the induction of Fos protein in cat visual cortex during

741   and after the critical period. *Molecular brain research*, *21*(1-2), 47-54.

742

743   Mower GD, Kaplan IV (2002). Immediate early gene expression in the visual cortex of

744   normal and dark reared cats: differences between fos and egr-1. *Molecular brain*

745   *research*, *105*(1-2), 157-160.

746

747   Niell CM, Stryker MP (2008). Highly selective receptive fields in mouse visual

748   cortex. *Journal of Neuroscience*, *28*(30), 7520-7536.

749

750   Niell CM, Stryker MP (2010). Modulation of visual responses by behavioral state in

751   mouse visual cortex. *Neuron*, *65*(4), 472-479.

752

753   Nowak LG, Azouz R, Sanchez-Vives MV, Gray CM, McCormick DA (2003).

754   Electrophysiological classes of cat primary visual cortical neurons in vivo as

755   revealed by quantitative analyses. *Journal of neurophysiology*, *89*(3), 1541-1566.

756

757   Pettigrew JD (1974). The effect of visual experience on the development of stimulus

758   specificity by kitten cortical neurones. *The Journal of physiology*, *237*(1), 49-74.

759

760   Rao RP, Ballard DH (1999). Predictive coding in the visual cortex: a functional

761   interpretation of some extra-classical receptive-field effects. *Nature*

762   *neuroscience*, *2*(1), 79-87.

763

764   Ringach DL (2009). Spontaneous and driven cortical activity: implications for
765   computation. *Current opinion in neurobiology*, *19*(4), 439-444.

766

767   Rosen KM, McCormack MA, Villa-Komaroff L, Mower GD (1992). Brief visual
768   experience induces immediate early gene expression in the cat visual
769   cortex. *Proceedings of the National Academy of Sciences*, *89*(12), 5437-5441.

770

771   Saleem AB, Ayaz A, Jeffery KJ, Harris KD, Carandini M (2013). Integration of visual
772   motion and locomotion in mouse visual cortex. *Nature neuroscience*, *16*(12),
773   1864.

774

775   Schmitzer-Torbert N, Jackson J, Henze D, Harris K, Redish AD (2005). Quantitative
776   measures of cluster quality for use in extracellular
777   recordings. *Neuroscience*, *131*(1), 1-11.

778

779   Schölvinck ML, Saleem AB, Benucci A, Harris KD, Carandini M (2015). Cortical state
780   determines global variability and correlations in visual cortex. *Journal of*
781   *Neuroscience*, *35*(1), 170-178.

782

783   Shadlen MN, Newsome WT (1998). The variable discharge of cortical neurons:
784   implications for connectivity, computation, and information coding. *Journal of*
785   *neuroscience*, *18*(10), 3870-3896.

786

787   Sheng M, Greenberg ME (1990). The regulation and function of c-fos and other

788   immediate early genes in the nervous system. *Neuron*, *4*(4), 477-485.

789

790   Sheng M, McFadden G, Greenberg ME (1990). Membrane depolarization and calcium

791   induce c-fos transcription via phosphorylation of transcription factor

792   CREB. *Neuron*, *4*(4), 571-582.

793

794   Shuler   MG,   Bear   MF   (2006).   Reward   timing   in   the   primary   visual

795   cortex. *Science*, *311*(5767), 1606-1609.

796

797   Stănişor L, van der Togt C, Pennartz CM, Roelfsema PR (2013). A unified selection

798   signal for attention and reward in primary visual cortex. *Proceedings of the*

799   *National Academy of Sciences*, *110*(22), 9136-9141.

800

801   Treue S (2001). Neural correlates of attention in primate visual cortex. *Trends in*

802   *neurosciences*, *24*(5), 295-300.

803

804   Tsodyks M, Kenet T, Grinvald A, Arieli A (1999). Linking spontaneous activity of single

805   cortical neurons and the underlying functional architecture. *Science*, *286*(5446),

806   1943-1946.

807

808   Turrigiano GG (2008). The self-tuning neuron: synaptic scaling of excitatory

809   synapses. *Cell*, *135*(3), 422-435.

810

811   Turrigiano GG, Nelson SB (2004). Homeostatic plasticity in the developing nervous

812   system. *Nature Reviews Neuroscience*, *5*(2), 97-107.

813

814   Vinck M, Batista-Brito R, Knoblich U, Cardin JA (2015). Arousal and locomotion make

815   distinct contributions to cortical activity patterns and visual

816   encoding. *Neuron*, *86*(3), 740-754.

817

818   Vinje WE, Gallant JL (2000). Sparse coding and decorrelation in primary visual cortex

819   during natural vision. *Science*, *287*(5456), 1273-1276.

820

821   Wissig SC, Kohn A (2012). The influence of surround suppression on adaptation effects

822   in primary visual cortex. *Journal of neurophysiology*, *107*(12), 3370-3384.

823

824

825   Yamada Y, Hada Y, Imamura K, Mataga N, Watanabe Y, Yamamoto M (1999).

826   Differential expression of immediate-early genes, c-fos and zif268, in the visual

827   cortex of young rats: effects of a noradrenergic neurotoxin on their

828   expression. *Neuroscience*, *92*(2), 473-484.

829

830   Zohary E, Shadlen MN, Newsome WT (1994). Correlated neuronal discharge rate and its

831   implications for psychophysical performance. *Nature*, *370*(6485), 140-143.

832

833   **Figure Legends**

834

835   **Figure 1.** Circadian L-D and D-L transitions have a small effect on V1 firing rates.

836   **A**, Experimental protocol. Single-unit recordings were obtained from juvenile rats for a

837   continuous 9-day period (P24-P32). Throughout this period animals were kept in a

838   regular 12h/12h light/dark cycle and thus underwent light-dark (L-D, purple arrows) and

839   dark-light (D-L, yellow arrows) transitions at regular 12-hour intervals. **B**, Left, average

840   waveform for each continuously recorded unit, identified as regular spiking unit (RSU,

841   red) or fast-spiking cell (FS, blue). Right, plot of trough-to-peak time vs waveform slope

842   0.4 ms after trough reveals the bi-modal distribution used to classify recorded units as

843   RSU or FS. **C**, Example raster plot of spiking activity for a recorded unit across several

844   days, showing 20 minutes of activity centered on the L-D (top) and D-L (bottom)

845   transitions. Blue bars represent the peri-event time histogram obtained by averaging

846   across days. **D**, Cumulative distributions of RSU firing rates averaged over the 10

847   minutes of light (solid line) or dark (dashed line) around the transitions, for L-D (left) and

848   D-L (right) transitions (L-D, $p = 0.875$; D-L, $p = 0.99$, two-sample Kolmogorov-Smirnov

849   test). **E**, As in D, but for FS units (L-D, $p = 0.99$; D-L $p = 1.0$, two-sample Kolmogorov-

850   Smirnov test). **F**, Mean firing rate for each RSU, averaged across all transitions

851   experienced by that neuron, in L-D (left) and D-L (right) transitions. Paired data indicates

852   the average FR is for the same neuron. Distributions were not significantly different (L-

853   D, $p = 0.677$; D-L, $p = 0.655$; Wilcoxon rank-sum test), but individual neurons across the

854   whole distribution showed consistent changes at the transitions (L-D, *** $p = 0.0002$; D-

855   L, **** $p < 0.0001$; Wilcoxon signed-rank test). **G**, as in F, but for FS units. Distributions

42

856   were not different (L-D, p = 0.905; D-L, p = 0.827; Wilcoxon rank-sum test), but

857   individual FS units changed their firing consistently at D-L, but not L-D transitions (L-D,

858   p = 0.318; D-L, * p = 0.026; Wilcoxon signed-rank test). *H*, Percent change in firing rate

859   across transition for RSUs (L-D, -7.09% ± 1.99%, *** p = 0.0006; D-L, 15.60% ±

860   4.00%, p = **** 0.0002; one-sample t-test). *I*, as H, for FS units. Percentage change in

861   FR was not different from 0 in either condition (L-D, -2.75% ± 3.80%, p = 0.475; D-L:

862   9.73% ± 5.12%, p = 0.067, one-sample t-test).

863

864 **Figure 2.** Changes in natural visual input modestly modulate the firing of V1 neurons

865 during wake but not sleep.

866 *A*, Comparison of mean firing rates, in 10-minute averages around the transitions, in L-D

867 and D-L transitions when the animal was awake for the whole 20 minutes. Activity in

868 light and dark was strongly correlated for both transition types. *B*, as in A, but for

869 transitions during which animals were asleep for the 20 minute period around the

870 transition. Firing rates in light and dark during sleep were also strongly correlated. *C*,

871 Mean firing rate of individual RSUs, calculated in 10-minute averages around luminance

872 transitions and averaged across all transitions during which animals were awake.

873 Neuronal activity changed consistently at the transitions (L-D, $p = 0.0001$; D-L, $p =$

874 0.0457; Wilcoxon signed-rank test). *D*, as in C, but for transitions during which animals

875 were asleep. No significant change was observed (L-D, $p = 0.656$; D-L, $p = 0.925$;

876 Wilcoxon signed-rank test). *E*, As in C, for FS units. Cells' activity only changed

877 significantly at D-L transitions (L-D, $p = 0.689$; D-L, $p = 0.039$; Wilcoxon signed-rank

878 test). *F*, As in D, for FS cells. No significant change was observed (L-D, $p = 0.557$; D-L,

879 $p = 0.638$; Wilcoxon signed-rank test).

880

44

881 **Figure 3.** A subset of RSUs consistently increase their firing rate in response to expected

882 dark-light transitions.

883 *A*, example of a RSU unresponsive to light transitions (left, L-D; right, D-L). Top, binned

884 firing rate for each transition; bottom, average across transitions. *B*, example RSU that

885 responds consistently to luminance transitions. *C*, Percentage of RSUs found to be

886 responsive to L-D (left) and D-L (right) transitions and bootstrap control. Black lines

887 show experimental value (actual % of responsive neurons); red line shows bootstrap

888 mean; light red bar shows extent of the bootstrap 95% confidence interval (L-D, actual

889 value: 6.25%, bootstrap mean: 3.55%; 95% CI: 0% - 12.62%; D-L, actual value: 14.06%;

890 bootstrap mean: 3.09%; 95% CI: 0% - 9.91%; n = 64). *D*, Mean firing rate averaged

891 across transitions for all D-L-responsive RSUs, calculated for two hour around each

892 transition for L-D (top) and D-L (bottom) transitions. The transient nature of the firing

893 rate response is visible in the bottom panel.

894

45

895   **Figure 4.** L-D and D-L transitions have no effect on V1 firing rates over short timescales.

896   *A*, Raster plot showing activity of one example RSU in a 10-second interval around L-D

897   and D-L transitions. Vertical ticks represent spikes, rows represent transitions happening

898   on different recording days. *B*, A second example RSU, showing a 30-second interval

899   around transitions. *C,* Mean ISI for all recorded cells, obtained by averaging ISIs in 10-

900   second bins around L-D and D-L transitions for different days. Each dot represents the

901   mean for one cell, obtained by averaging across days. No significant change was

902   observed (L-D, p = 0.97; D-L, p = 0.31; Wilcoxon sign-rank test). *D*, As in C, but for 1-

903   second averages. No significant change was observed (L-D, p = 0.27; D-L, p = 0.36;

904   Wilcoxon sign-rank test).

905

46

906   **Figure 5.** Randomly timed L-D and D-L transitions induce consistent firing rate changes

907   in RSUs.

908   *A*, Experimental design. Animals were exposed to 10-minute periods of darkness during

909   the light phase, and 10-minute periods of light during the dark phase, at random points

910   throughout the light/dark cycle. Mean firing rates were calculated in 10-minute intervals

911   around the transition. *B,* Percentage of RSUs that were responsive to luminance

912   transitions, when transitions happened in epochs of sleep. Black line shows actual

913   experimental value; red line shows bootstrap mean; light red bar covers the bootstrap

914   95% confidence interval (sleep, L-D: 21.9%, bootstrap mean and 95% CI: 4.42% [0% -

915   8.95%], n=64; D-L: 13.4%, bootstrap mean and 95% CI: 4.31% [0% - 9.38%], n=67). *C*,

916   as in B, but for transitions happening while animals were awake (wake, L-D: 17.6%,

917   bootstrap mean and 95% CI: 4.22% [0% - 8.79%], n=91; D-L: 12.7%, bootstrap mean

918   and 95% CI: 4.33% [0% - 9.09%], n=55).

919

920

921   **Figure 6.** Pairwise correlations in V1 are higher during light than during dark.

922   *A*, Example pairwise correlation structure of 30 neurons from a single animal during light

923   (left; calculated over the 12-hour period at P27) and during dark (right; calculated over

924   the 12-hour period at P27.5). *B*, The average correlation of 922 pairs from five animals

925   over 4 days, normalized to the average correlation of each animal relative to P26 in light.

926   The gap in the data at P26 corresponds to the time animals were anesthetized for

927   monocular deprivation, which was excluded from analysis. *C*, Comparison of the average

928   correlation of 922 pairs during light and during dark with bin size 5ms (left) and bin size

929   100ms (right). (left: $p < 10^{-70}$; right: $p < 10^{-125}$, Wilcoxon signed-rank test). *D*,

930   Comparison of average correlation of 922 pairs in wake during light and during dark with

931   bin size 5ms (left) and bin size 100ms (right). (left: $p < 10^{-55}$; right: $p < 10^{-110}$,

932   Wilcoxon signed-rank test).

933

934

935

48

936 **Figure 7.** Prolonged darkness results in increased *c-fos* expression upon light re-

937 exposure.

938 *A*, Experimental protocol. Animals were exposed to either a regular 12h/12h light/dark

939 cycle, and sacrificed 1 hour after lights on at P29 (regular control, RC, n = 22 slices, 4

940 animals); exposed to darkness for 60 hours starting at P26 and sacrificed before lights on

941 (dark control, DC, n = 23 slices, 4 animals); exposed to 60 hours of darkness starting at

942 P26 and sacrificed 1 hour after light re-exposure (light exposed, LE, n = 28 slices, 5

943 animals). *B*, representative images showing DAPI (top row) and *c-fos* (bottom row)

944 immunostaining for regular control (left), dark control (middle), and light exposed (right)

945 animals. *C*, Percentage of *c-fos*-positive cells in all three groups (RC: 11.4% ± 1.6%; DC:

946 6.1% ± 0.8%; LE: 16.8% ± 1.7%. * p=0.032; *** p=0.001, one-way ANOVA with Tukey

947 post-hoc test). *D*, Total co-localized DAPI and c-fos staining intensity, normalized to

948 average of RC group (RC: 1.00 ± 0.06; DC: 0.79 ± 0.05; LE: 1.31 ± 0.09; * p=0.011; ***

949 p=0.001, one-way ANOVA with Tukey post-hoc test).

950

951

49

952   **Figure 8.** Light re-exposure after prolonged darkness causes a robust and widespread

953   increase in V1 firing, following a slight reduction in firing rates over the dark period.

954   *A*, Time course of RSU and FS spiking in a 2-hour period around the time of light re-

955   exposure. Individual unit traces (top) and average across cells (bottom) shows marked

956   increase in firing at the time of lights on. *B*, Percentage change in firing rate between the

957   10 minutes prior to and the 10 minutes immediately following light re-exposure (all cells,

958   87.1% ± 13.5%, n=44, **** $p < 10^{-7}$; RSU, 80.7% ± 14.9%, n=32, *** $p < 10^{-5}$; FS,

959   104.3% ± 29.8%, n=12, ** p = 0.005; one-sample t-test). *C*, Mean firing rate in the 10

960   minutes before and after the transition, for each recorded RSU (**** $p < 10^{-5}$, Wilcoxon

961   signed-rank test). *D*, As in C, for recorded FS cells (* p = 0.034, Wilcoxon signed-rank

962   test). *E*, Mean firing rate for all recorded RSUs, averaged across the first 12-hour period

963   within the 60 hours of darkness (First 12h, mean ± s.e.m: 4.00 ± 0.97 Hz, median: 1.18

964   Hz, n = 47) and the last 12-hour period of darkness before light re-exposure (Last 12h,

965   mean ± s.e.m: 2.27 ± 0.57 Hz, median: 0.85 Hz, n = 55; * p = 0.044, Wilcoxon rank-sum
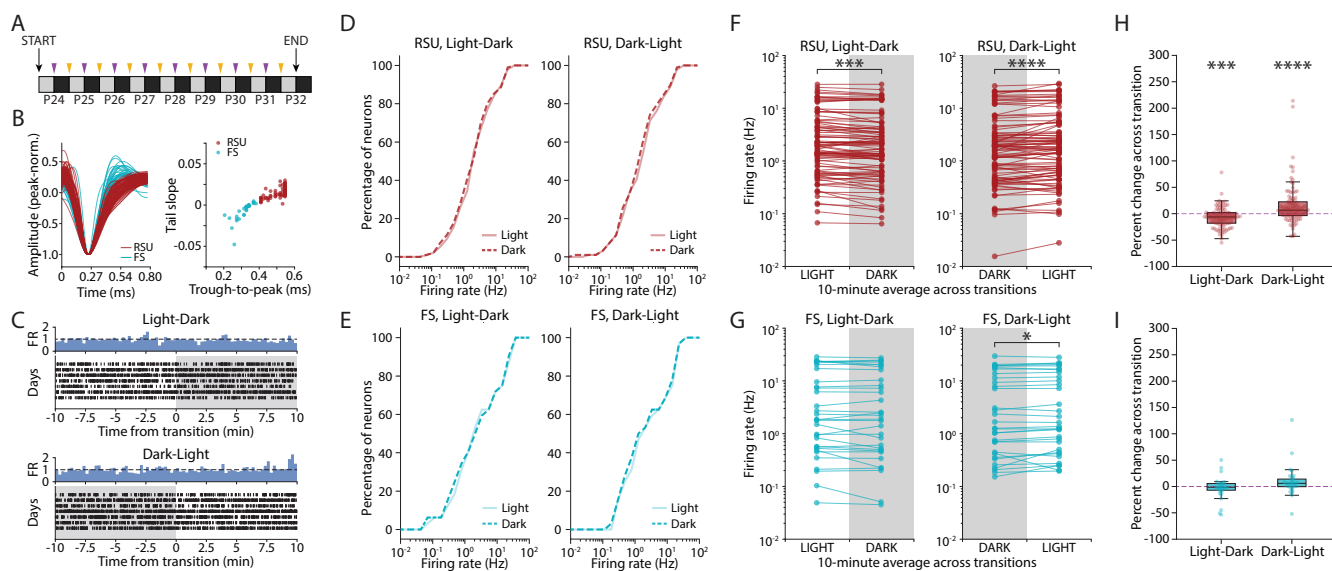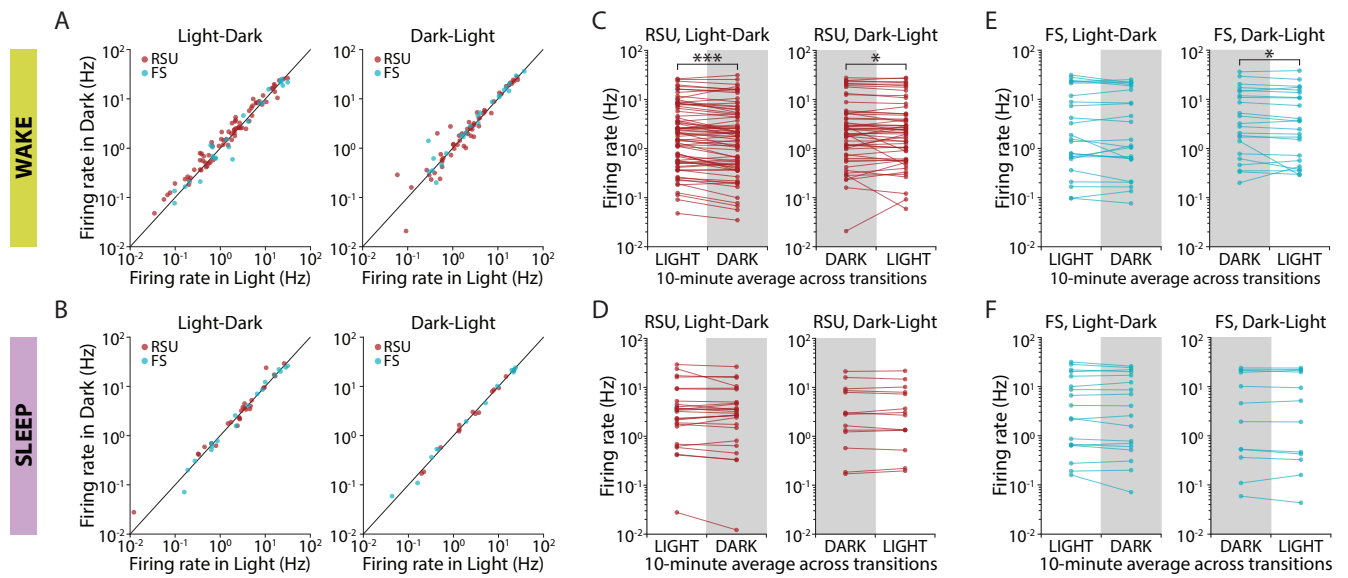
966   test).
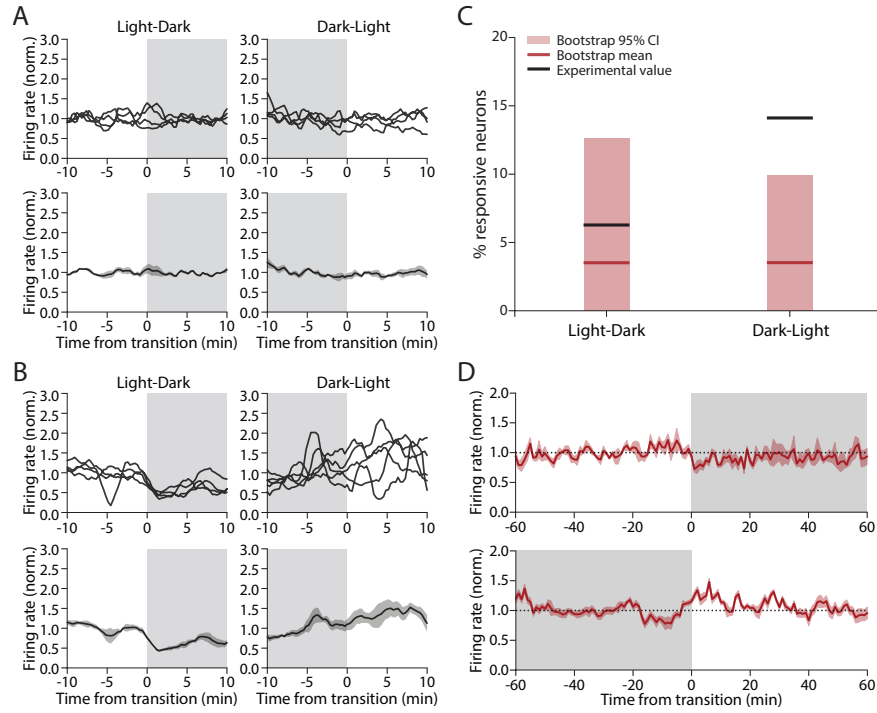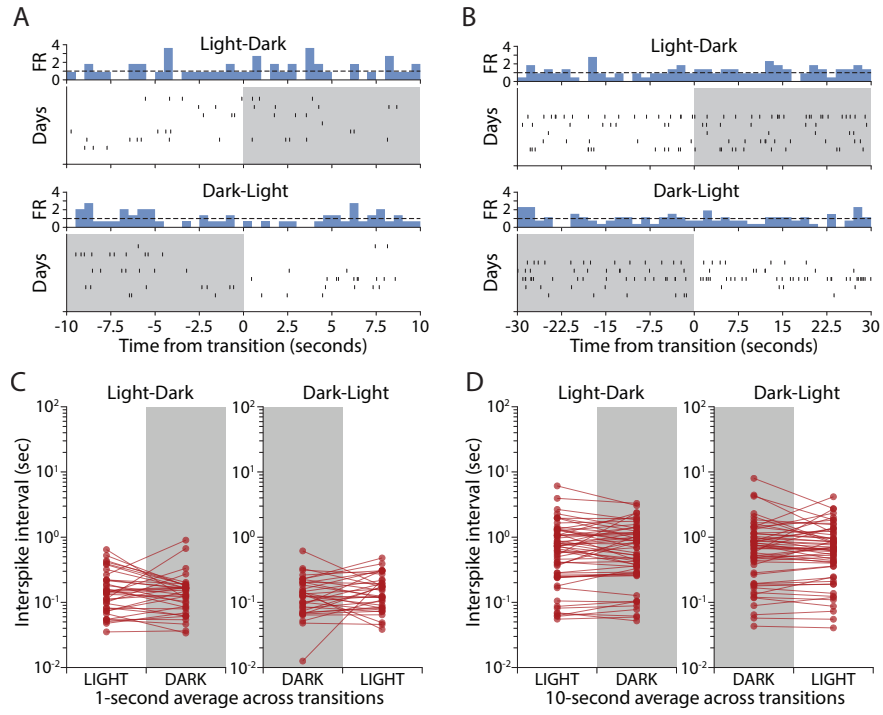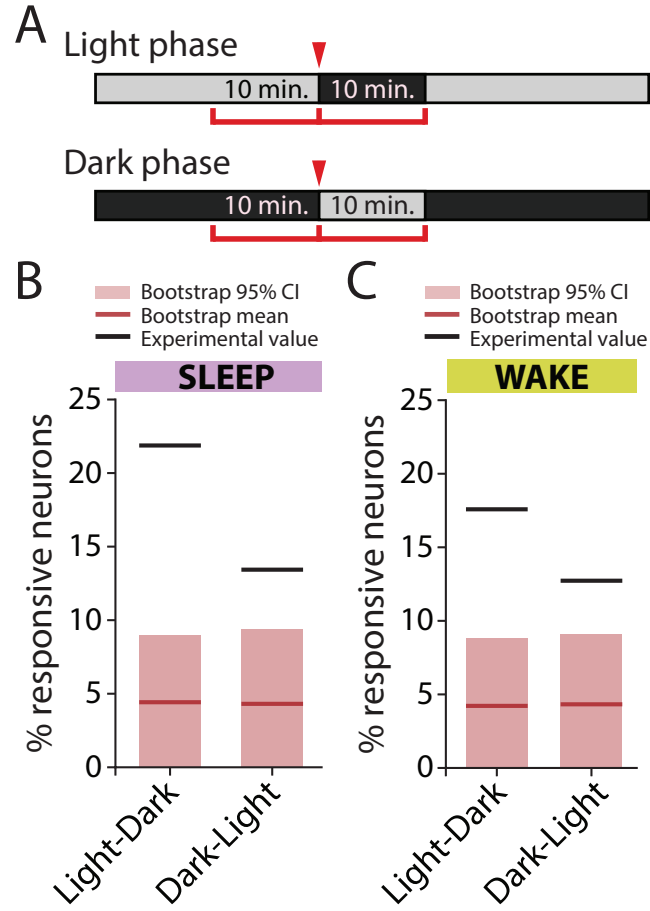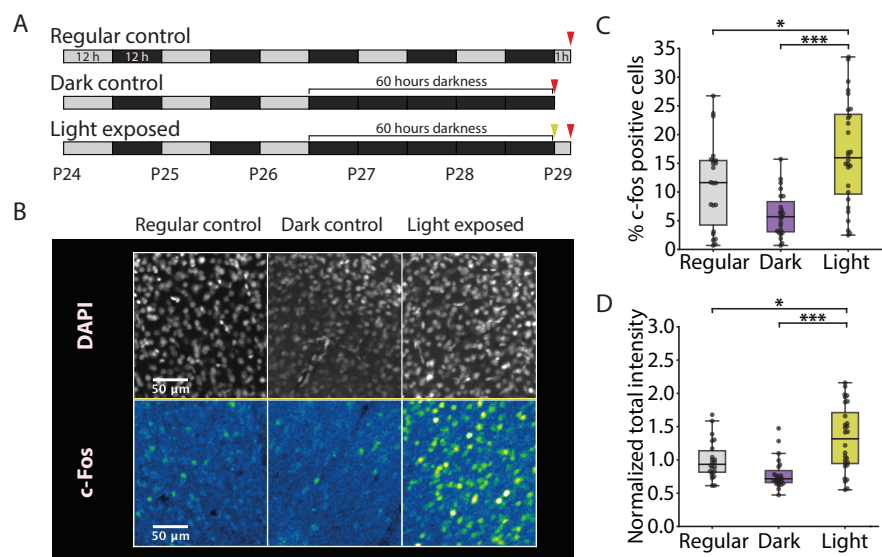
967

Figure 1

Figure 2

Figure 3

Figure 4

Figure 5

Figure 6

Figure 7

Figure 8